N- vs. C-Domain Selectivity of Catalytic Inactivation of Human Angiotensin Converting Enzyme by Lisinopril-Coupled Transition Metal Chelates

Lalintip Hocharoen[1], **Jeff C. Joyner**[1,2,3], and **J. A. Cowan**[1,2,3,*]

[1]Evans Laboratory of Chemistry, Ohio State University, 100 West 18th Avenue, Columbus, Ohio 43210

[2]The Ohio State Biochemistry Program, 784 Biological Sciences 484 W. 12th Avenue, Columbus, Ohio 43210

[3]MetalloPharm LLC, 1790 Riverstone Drive, Delaware, OH 43015

Abstract

The N- and C-terminal domains of human somatic Angiotensin I Converting Enzyme (sACE-1) demonstrate distinct physiological functions, with resulting interest in the development of domain-selective inhibitors for specific therapeutic applications. Herein, the activity of lisinopril-coupled transition metal chelates were tested for both reversible binding and irreversible catalytic inactivation of sACE-1. C/N domain binding selectivity ratios ranged from 1 to 350, while rates of irreversible catalytic inactivation of the N- and C-domains were found to be significantly greater for the N-domain, suggesting a more optimal orientation of the M-chelate-lisinopril complexes within the active site of the N-domain of sACE-1. Finally, the combined effect of binding selectivity and inactivation selectivity was assessed for each catalyst (double-filter selectivity factors), and several catalysts were found to cause domain-selective catalytic inactivation. The results of this study demonstrate the ability to optimize the target selectivity of catalytic metallopeptides through both binding and orientation factors (double-filter effect).

Keywords

catalytic inactivation; domain selectivity; double-filter effect; metallopeptide; metal chelate; lisinopril; angiotensin converting enzyme

INTRODUCTION

Angiotensin I Converting Enzyme (ACE) is involved in the Renin-Angiotensin System (RAS) and plays an essential role in the regulation of blood pressure and fluid homeostasis.[1–3] The action of ACE in the maintenance of homeostasis occurs through the cleavage of angiotensin I to form angiotensin II, a potent vasoconstricting octapeptide. Angiotensin II causes blood vessels to constrict, leading to increased blood pressure.[3–5] Additionally, ACE promotes degradation of the vasodepressor peptide bradykinin, and this cleavage further increases blood pressure.[5–8] Because of its prominent physiological roles, ACE has become an attractive therapeutic target for the treatment of hypertension and heart failure.

Human ACE is a glycoprotein and primarily a membrane-bound ectoenzyme that is expressed as a somatic isoform (sACE-1) and a testis isoform (tACE).[9] Human sACE-1 contains two similar extracellular domains, the N- and C-domains, each containing a conserved Zn^{2+}-binding motif HEXXH at the active site.[10,11] Human tACE is identical to the C-domain of sACE-1, except for the first 36 N-terminal residues.

Although the N- and C-domains share $\sim 60\%$ sequence homology, previous research has shown notable differences in the substrate specificity, sensitivity to chloride activation, inhibitor-binding affinity and physiological roles for the two domains.[12–17] The N-domain has activity that is less dependent on chloride activation[12,18] and is more thermostable than the C-domain of sACE-1.[19] While both domains possess similar affinity for the substrates angiotensin I, substance P, and bradykinin,[12] the N-domain of sACE-1 specifically cleaves angiotensin-(1–7),[20] luteinizing hormone-releasing hormone (LH-RH),[12] enkephalin precursor Met-Enk-Arg-Phe,[20] and natural tetrapeptide Acetyl-Ser-Asp-Lys-Pro.[21–23] However, studies using the N-domain-selective inhibitor, phosphinic peptide Ac-Asp-$_{(L)}$Pheψ(PO$_2$-CH$_2$)$_{(L)}$Ala-Ala-NH$_2$ **1** (RXP407),[15,24] showed no effect on blood pressure regulation, consistent with studies on transgenic mice, in which overexpression of only the N-domain gave a phenotype that was similar to that for transgenic mice in which the entire *ACE* gene was knocked out These results suggest that the N-domain is unlikely to be involved in cardiovascular function. However, other studies have demonstrated distinct and significant roles for the N-domain such as control of hematopoietic stem cell proliferation. The C-domain of sACE-1 has been proposed to be the most prominent domain in the regulation of blood pressure, consistent with the fact that lisinopril has been shown to favorably bind to the C-domain of sACE-1 and is a commercially available drug for the treatment of hypertension. The development of drugs selective for either the N- or C-domain could be beneficial for specific therapeutic treatments and/or experimental strategies.

Although there already exist several domain-selective inhibitors of sACE-1, such as the phosphinic peptides **1** and (2S)-2-[[2-[hydroxy-[(1R)-2-phenyl-1-(phenylmethoxycarbonylamino)ethyl] phosphoryl]cyclopentanecarbonyl]amino]-3-(1H–indol-3-yl)propanoic acid (RXPA 380),[17] these inhibitors function through a reversible mode of inhibition, requiring stoichiometric saturation of sACE-1. We have been developing a series of catalytic metallopeptides that *irreversibly* inactivate sACE-1, without the requirement for target saturation (potentially reducing side-effects for *in vivo* use, relative to

reversible inhibitors). These compounds each contain a catalytic metal-chelate, such as the M-ATCUN (amino terminal copper/nickel binding motif), M-DOTA, M-EDTA, or M-NTA complexes, where $M = Fe^{3+}$, Co^{2+}, Ni^{2+} or Cu^{2+}, coupled to lisinopril, which serves as the targeting ligand that binds sACE-1 with high affinity. Such catalytic metallopeptides were previously shown to promote oxidative modification and/or cleavage of targeted proteins or nucleotides through multiple-turnover production of reactive oxygen species (ROS).[25–30] Our previous study demonstrated that lisinopril-conjugated transition metal-chelates, consisting of combinations of the transition metals Fe^{3+}, Co^{2+}, Ni^{2+}, and Cu^{2+} and the chelators EDTA-lisinopril, NTA-lisinopril, DOTA-lisinopril, and tripeptide GGH-lisinopril, were able to both reversibly inhibit and irreversibly modify and/or cleave sACE-1 in the presence of ascorbate, O_2 and/or peroxide. However, the domain selectivity of their reversible inhibition and irreversible inactivation and/or cleavage could not be assessed by the previous methods.

The goal of the current study was to characterize the N- vs. C-domain selectivity for both reversible inhibition (binding selectivity) and irreversible inactivation (catalytic selectivity) of sACE-1 that were mediated by metal-chelate-lisinopril catalysts. In order to study individual domains, we monitored sACE-1 activity using the commercially available fluorogenic substrates Abz-SDK(Dnp)P-OH, derived from tetrapeptide Ac-SDKP, and Abz-LFK(Dnp)-OH, obtained from a combinatorial library, which are selective for the N- and C-domains of sACE-1, respectively. Abz-SDK(Dnp)P-OH is selectively hydrolyzed by the N-domain of sACE-1 with a k_{cat}/K_M that is 50-fold higher than observed for hydrolysis by the C-domain,[22] while Abz-LFK(Dnp)-OH is cleaved by the C-domain with a k_{cat}/K_M that is 75-fold higher than observed for the N-domain.[31] Therefore, the separate use of each domain-selective substrate allowed us to assess the reversible inhibition and irreversible inactivation of each corresponding domain in an isolated manner. A similar approach was used previously by Jullien *et al*. to assess the domain selectivity of several reversible inhibitors of sACE-1.[16] In addition to the M-chelate-lisinopril complexes mentioned above, we also present results herein for novel catalysts based on combinations of the metals Fe^{3+}, Ni^{2+}, and Cu^{2+}, with lisinopril-coupled 4,11-bis(carboxymethyl)-1,4,8,11 tetraazabicyclo[6.6.2]hexadecane 4,11-diacetic acid (CB-TE2A-lisinopril). All complexes are shown in Figure 1. To assess the C/N-domain selectivity for each catalyst, we have evaluated binding affinity (K_i) and the inactivation rates for each domain of sACE-1. Furthermore, we have established C/N double-filter selectivity factors that both account for the overall reactivity of the catalysts, and provide an approach for screening the candidates for the domain-selective irreversible inactivation of sACE-1 and other protein targets.

RESULTS

Preparation and Characterization of Lisinopril-Coupled Transition Metal Chelates

The chelators used in these studies (EDTA, NTA, DOTA, GGH and CB-TE2A) were purchased from commercial companies and coupled to the side chain of lisinopril as previously described.[33] The identities and purity of the synthesized chelate-lisinopril compounds were validated as previously reported, with > 99% purity as defined by RP-HPLC and ESI-MS.[33]

Determination of Michaelis-Menten Kinetic Parameters for Cleavage of Domain-Selective Substrates

sACE-1 hydrolyzes the fluorogenic substrates Abz-SDK(Dnp)P-OH and Abz-LFK(Dnp)-OH at the D-K and L-F peptide bonds, respectively.[22,31] Variable concentrations of each domain-selective substrate were incubated with sACE-1 (1 nM), and cleavage of substrate was immediately monitored by real-time fluorimetry. The k_{cat}, K_M and k_{cat}/K_M values were obtained from Michaelis-Menten plots (summarized in Table 1). The values were also compared to those for the generic substrate used in our previous study, Mca-RPPGFSAFK(Dnp)-OH, which is derived from bradykinin and lacks significant domain selectivity.[30]

Determination of IC$_{50}$ Values

Dose-dependent inhibition of each domain of sACE-1 by each M-chelate-lisinopril species was monitored by incubating sACE-1 with variable concentrations of each complex at 37°C for 20 min, prior to mixing with each domain-selective fluorogenic substrate. The M-chelate-lisinopril complexes studied were M-NTA-lisinopril, M-GGH-lisinopril, M-EDTA-lisinopril, M-DOTA-lisinopril and M-CB-TE2A-lisinopril, where M = Fe^{3+}, Co^{2+}, Ni^{2+} and Cu^{2+}. Neither Fe-GGH-lisinopril nor Co-CB-TE2A-lisinopril were used in the experiments due to weak metal binding, as shown in the metal titration profiles (Supporting Information). The IC$_{50}$ curves for lisinopril and each chelate-lisinopril complex are shown in Figure 2, for each domain-selective substrate. Lisinopril gave the lowest IC$_{50}$ values (1.5 and 0.25 nM for the N- and C-domain, respectively). The attachment of chelators to the lysine side chain of lisinopril resulted in increased IC$_{50}$ values ranging from 20 to 2700 nM and from 0.6 to 630 nM for the N- and C-domain of sACE-1, respectively. The IC$_{50}$ values appeared to increase with the size of the chelate-lisinopril complexes: NTA-lisinopril < GGH-lisinopril < EDTA-lisinopril < CB-TE2A-lisinopril < DOTA-lisinopril. An exception was observed for CB-TE2A-lisinopril. Although the mass of CB-TE2A-lisinopril (~728 amu) is between that of EDTA-lisinopril and DOTA-lisinopril, it demonstrated a very low IC$_{50}$ value, comparable to IC$_{50}$ values for the M-NTA-lisinopril complexes. Additionally, IC$_{50}$ values appeared to increase with the negative charge of the attached chelator.

When using the N-domain-selective substrate, Abz-SDK(Dnp)P-OH, the IC$_{50}$ values ranged from 20 to 3400 nM, in the order M-NTA-lisinopril ≈ M-CB-TE2A-lisinopril < M-GGH-lisinopril < M-EDTA-lisinopril ≈ M-DOTA-lisinopril. When using the C-domain-selective substrate, Abz-LFK(Dnp)-OH, the IC$_{50}$ values were generally lower than those obtained for the N-domain-selective substrate. The IC$_{50}$ values (and K_i values) for the C-domain-selective substrate ranged from 0.2 to 900 nM and increased in the order M-NTA-lisinopril < M-GGH-lisinopril < M-CB-TE2A-lisinopril < M-EDTA-lisinopril ≈ M-DOTA-lisinopril. The overall trends observed using domain-selective substrates were generally in agreement with our previous observations of positive correlations between the IC$_{50}$ value and both the negative charge and the size of M-chelate-lisinopril complexes (shown in Figure 3).

Inhibition Mode by Dixon Plots and Inhibition Constants

To determine whether the M-chelate-lisinopril complexes bound directly to the active site of each domain of sACE-1, the concentrations of each substrate and selected complex were

varied, and Dixon plots were constructed. Cu-GGH-lisinopril and lisinopril were used as representative complexes. As shown in Figure 4, lisinopril, a competitive inhibitor, gave a Dixon plot in which the fits of various concentrations of Abz-LFK(Dnp)-OH intersected within the left quadrant. A similar Dixon plot profile was observed for Cu-GGH-lisinopril, suggesting that both lisinopril and Cu-GGH-lisinopril also behave as competitive inhibitors of the C-domain of sACE-1 (in the absence of co-reactants). We also demonstrated that both lisinopril and Cu-GGH-lisinopril bound directly to the active site of the N-domain of sACE-1, using the same approach with Abz-SDK(Dnp)P-OH (Supporting Information). In summary, both lisinopril and Cu-GGH-lisinopril act as competitive inhibitors of both domains of sACE-1, although with differing affinities (Table 2).

Inhibition constants (K_i) for each M-chelate-lisinopril complex at both N- and C-domains were obtained by use of the IC_{50} values for each complex, the concentration of substrates, and K_M for the corresponding substrate, as shown in eqn. 4 (Experimental Section). A summary of the IC_{50} and K_i values obtained for each M-chelate-lisinopril complex for both the N- and C-domains, is shown in Table 2. The K_i values determined for lisinopril were 1 and 0.1 nM for the N- and C-domain, respectively, consistent with previous reports.[30,34] For the M-chelate-lisinopril complexes, K_i values obtained from the C-domain-selective substrate ranged from 2 to 200-fold lower than the corresponding K_i values obtained for the N-domain-selective substrate. However, M-CB-TE2A-lisinopril showed a similar affinity to both domains, with a $K_i \sim 20$ nM, with the exception of Fe-CB-TE2A-lisinopril, which showed a higher K_i value for binding to the N-domain of sACE-1. In general, complexes showed selectivity toward the C-domain, consistent with the C-domain selectivity of lisinopril.

Each domain selectivity ratio (C/N) listed in Table 2 was obtained from the ratio of the K_i for the N-domain to the K_i for the C-domain for each complex. A comparison of the C/N domain selectivity ratio and the size, charge, and identity of the side chain of each lisinopril complex is illustrated in Figure 5. The NTA-lisinopril complexes demonstrated the highest C/N selectivity ratio, while the CB-TE2A-lisinopril complexes showed the lowest C/N domain selectivity ratio (except for Fe-CB-TE2A-lisinopril). The C/N domain selectivity appeared to decrease with higher mass of the M-chelate-lisinopril complexes, with the exception of lisinopril (no attached M-chelate). For M-CB-TE2A-lisinopril, alternative factors, such as hydrophobicity may have influenced the result; CB-TE2A-lisinopril appears to be more hydrophobic than the other chelate-lisinopril species, as evidenced by a comparatively higher retention time in RP-HPLC (Figure SM1 of the Supporting information). Among the same metal binding domains, varying the transition metal typically did not introduce significant variability in the C/N domain selectivity (except for Fe-CB-TE2A-lisinopril).

Time-Dependent Inactivation of sACE-1

Reactions were performed that contained sACE-1, M-chelate-lisinopril complex, and co-reactants (H_2O_2, ascorbate, H_2O_2+ascorbate, or none). A concentration of each M-chelate-lisinopril complex that gave approximately 80% sACE-1 activity (for each substrate) was used (see Supporting Information for concentrations). At specific time points, the enzyme

activity at one of the two domains was assayed by mixing aliquots from the reaction with the corresponding domain-selective fluorogenic substrate. The remaining activity of sACE-1 at each time point during the incubation was obtained from the initial rate of substrate cleavage. All experiments were performed for each domain.

Time-dependent inactivation was observed for several M-chelate-lisinopril complexes. For the N-domain-selective substrate, under oxidative conditions (both H_2O_2 and ascorbate present), Cu-GGH-lisinopril showed the greatest inactivation rate followed by Co-EDTA-lisinopril $\approx$ Cu-EDTA-lisinopril > Ni-CB-TE2A-lisinopril > Cu-DOTA-lisinopril $\approx$ Fe-DOTA-lisinopril $\approx$ Cu-CB-TE2A-lisinopril > Co-DOTA-lisinopril $\approx$ Fe-CB-TE2A-lisinopril > Ni-EDTA-lisinopril > Ni-GGH-lisinopril > Co-GGH-lisinopril. In the presence of ascorbate (no H_2O_2), only Cu-GGH-lisinopril showed significant catalytic inactivation of sACE-1. In the presence of H_2O_2 (no ascorbate), rates of sACE-1 inactivation decreased in the order Co-EDTA-lisinopril > Fe-DOTA-lisinopril > Co-DOTA-lisinopril > Cu-GGH-lisinopril > Cu-EDTA-lisinopril > Ni-CB-TE2A-lisinopril > Ni-GGH-lisinopril. In the absence of co-reactants, the rates of sACE-1 inactivation for each complex were below background. Control experiments, in which no catalyst was present, were also conducted, and the inactivation rates were negligible (see Supporting Information).

For the C-domain-selective substrate, observed rates of sACE-1 inactivation were generally lower than for the N-domain-selective substrate. The fastest rate of inactivation of the C-domain of sACE-1 was observed for Co-EDTA-lisinopril, in the presence of H_2O_2 (no ascorbate). Both Cu-DOTA-lisinopril and Fe-DOTA-lisinopril also demonstrated relatively high inactivation rates when only H_2O_2 was present. In the presence of both H_2O_2 and ascorbate, the inactivation rates decreased in the order Co-EDTA-lisinopril > Ni-CB-TE2A-lisinopril > Cu-CB-TE2A-lisinopril > Cu-EDTA-lisinopril $\approx$ Fe-DOTA-lisinopril > Ni-EDTA-lisinopril > Cu-GGH-lisinopril $\approx$ Cu-DOTA-lisinopril $\approx$ Fe-CB-TE2A-lisinopril. In the presence of ascorbate (no H_2O_2), Cu-GGH-lisinopril showed the most prominent rate of catalytic inactivation, followed by Cu-EDTA-lisinopril, Co-GGH-lisinopril, and Ni-GGH-lisinopril. The rates of inactivation of sACE-1 by all M-chelate-lisinopril complexes, for both Abz-SDK(Dnp)P-OH and Abz-LFK(Dnp)-OH substrates, are plotted in Figure 6. A comparison of the rates of inactivation for the two substrates indicates the relative rates of inactivation of the N-domain vs. the C-domain (R_N and R_C, respectively).

DISCUSSION

Kinetic Parameters for Domain-Selective Substrates

sACE-1 contains two homologous domains that have different substrate selectivity. Prior studies have demonstrated that the natural tetrapeptide Ac-SDKP was cleaved selectively by the N-domain ($k_{cat}/K_M \sim 30\ \mu M^{-1}\ min^{-1}$ for the N-domain vs. $k_{cat}/K_M \sim 0.6\ \mu M^{-1}\ min^{-1}$ for the C-domain).[22] Due to the high efficiency of cleavage by the N-domain relative to the C-domain, we used the fluorogenic substrate Abz-SDK(Dnp)P-OH, derived from the natural tetrapeptide, in order to study the effect of the M-chelate-lisinopril complexes toward the N-domain of sACE-1.

The C-domain-selective fluorogenic substrate Abz-LFK(Dnp)-OH was obtained from a combinatorial study, in which it was shown that the substrate was cleaved selectively by the C-domain ($k_{cat}/K_M \sim$ 30 and 2200 μM^{-1} min^{-1} for the N- and C-domain, respectively).[31] Therefore Abz-LFK(Dnp)-OH was used as a C-domain-selective substrate for this work.

We determined the kinetic parameters for cleavage of each substrate by use of Michaelis-Menten plots (Supporting Information). The K_M and k_{cat} values were 35 ± 5 μM and 175 ± 10 min^{-1}, respectively, for cleavage of the N-domain-selective substrate, and 12 ± 2 μM and 1380 ± 90 min^{-1}, respectively, for cleavage of the C-domain-selective substrate. Our K_M values for these two substrates were comparable to other published results (41 and 4 μM for the N- and C-domain-selective substrates, respectively).[22,31] However, the catalytic activities were moderately lower, most likely reflecting the addition of Brij-35, which was shown to maintain enzyme stability, or the higher concentration of NaCl (300 mM) used in our experiments. In the absence of Brij-35, the activity of sACE-1 decreased over time (Supporting Information). It is not known exactly how Brij-35 stabilizes sACE-1; however, it has been proposed that this nonionic surfactant may provide hydrophobic interactions with the protein, resulting in preservation of the protein structure and/or solubility in aqueous solution (or preventing it from degradation).[35,36] On the other hand, Brij-35 may interact with the substrate, possibly leading to shifts in the apparent activity.

Domain-Selective Reversible Inhibition

Each M-chelate-lisinopril complex was tested for dose-dependent inhibition of each domain of sACE-1 (IC_{50} values). To compare the binding affinity of each complex for the two domains, K_i values for each domain were calculated as described earlier. The K_i values obtained using the N-domain-selective substrate were generally higher than those obtained using the C-domain-selective substrate (Table 2), suggesting that the complexes typically bind more favorably to the C-domain, with different degrees of C/N domain selectivity.

The sACE-1 binding affinity of the M-chelate-lisinopril complexes appeared to increase with a higher positive charge on the M-chelate centers of the complexes. A previous surface potential study revealed that the N-domain binding groove of sACE-1 is less negatively charged than that of the C-domain.[37] Therefore some of the M-chelate-lisinopril complexes with a higher positive charge showed tighter binding to the C-domain (lower K_i values) although other factors, such as size, also influenced the domain selectivity. M-NTA-lisinopril and M-CB-TE2A-lisinopril are good examples. The M-CB-TE2A-lisinopril complexes were found to bind both domains of sACE-1 with similar affinity, except for Fe-CB-TE2A-lisinopril, which favored the C-domain, most likely as a result of greater electrostatic attraction to the more negatively-charged binding groove of the C-domain. In general, the affinities for each domain were found to inversely correlate with the size (expressed as mass) of the M-chelate-lisinopril complexes. DOTA-lisinopril and EDTA-lisinopril are bulky, relative to other M-chelate-lisinopril complexes studied, and have a greater difficulty fitting into the active site of sACE-1, as reported in our previous study, resulting in higher K_i values.[30] However, the M-CB-TE2A-lisinopril complexes were an exception. The sizes of these complexes are between that of the M-EDTA-lisinopril and M-DOTA-lisinopril complexes, yet they had a greater affinity for both domains of sACE-1,

most likely because of their greater positive charge and relative hydrophobicity, as observed by a greater retention time in RP-HPLC purification (Supporting Information). A number of studies on peptide-based inhibitors of sACE-1 have demonstrated that a motif containing X-Proline, where X was a hydrophobic amino acid residue, was a lead structure for food-derived peptide inhibitors against ACE (Ile-Pro-Pro has an IC_{50} value of 5μM and lowers blood pressure by up to ∼ 30 mmHg in SHR)[38] due to a hydrophobic pocket in the active sites of sACE-1 formed by Tyr520/486, Phe457/423 and Phe527/453 (numbers correspond to N-domain/tACE).[38–40]

The C/N domain binding selectivity was obtained for each complex from the ratio of K_i values obtained using the N- and C-domain-selective substrates. The greatest C/N selectivity was observed for the M-NTA-lisinopril complexes, which have a less negative charge than the M-DOTA-lisinopril or M-EDTA-lisinopril complexes and have two empty *cis*-metal-coordination sites that may interact with specific amino acid residues within the C-domain binding groove, which is more negatively charged. These factors may contribute to the distinct domain selectivity of the M-NTA-lisinopril complexes. Interestingly, M-GGH-lisinopril, M-EDTA-lisinopril and M-DOTA-lisinopril all showed modest C-domain selectivity; their C/N selectivities were similar to that of free lisinopril, with the exception of Cu-GGH-lisinopril, which showed a greater C/N selectivity, possibly as a result of available axial metal-coordination sites within its square-planar geometry. The M-EDTA-lisinopril and M-DOTA-lisinopril complexes do not have an empty-coordination that could interact with residues in the C-domain.

Domain-Selective Irreversible Inactivation

Time-dependent catalytic inactivation of sACE-1 by the M-chelate-lisinopril complexes was monitored for each domain of sACE-1, and different rates of inactivation were observed. In the absence of redox co-reactants, the M-chelate-lisinopril complexes behaved as classical inhibitors–no time-dependent inactivation was observed. However, when ascorbate and/or H_2O_2 were added, a catalyst-promoted time-dependent decrease in the activity of sACE-1 was observed. As we reported previously, the M-chelate-lisinopril complexes facilitate the conversion of the oxidant O_2 (or H_2O_2) to reactive oxygen species (ROS), possibly via metal-bound intermediates, through single-electron transfer events.[41,42]

Additionally, ascorbate, a known pro-oxidant, reduces the oxidized metal centers, thereby creating a complete cycle of oxidation/reduction at the metal center.[42–44] Consequently, ROS can be produced with multiple turnover number, and this reactivity is optimal when the M-chelate reduction potential is poised between the reduction potentials of the reductant and oxidant half-reactions. This effect was observed in cases of oxidative catalytic cleavage of nucleic acids and/or inactivation of proteins.[26,29,44] However, we observed previously that the Cu-GGH-lisinopril complex, which has a much greater E^o (∼1000 mV), was the most efficient catalyst for the inactivation of sACE-1, suggesting a unique mechanism of ROS generation and/or protein inactivation.

Regarding the domain selectivity of irreversible catalytic inactivation, each domain was differently inactivated by each of the M-chelate-lisinopril complexes, as illustrated in Figure 6. The rates of catalytic inactivation of the N-domain were typically greater than those

observed for the C-domain, possibly due to either more favorable alignment of reactive metal centers within the N-domain or differing rates of association/dissociation of the complexes to/from each domain of sACE-1. For catalytic inactivation of the N-domain of sACE-1, a number of complexes had relatively high inactivation rates, including Cu-GGH-lisinopril, Co-EDTA-lisinopril, Cu-EDTA-lisinopril, and Fe-DOTA-lisinopril, and their ability to inactivate sACE-1 was dependent on the presence of co-reactants. Catalytic inactivation of both domains by Cu-GGH-lisinopril appeared to depend on O_2, since the highest inactivation rates were observed in the presence of ascorbate (the addition of H_2O_2, a mechanistic shunt, did not increase the inactivation rate). The catalysts Co-EDTA-lisinopril and Fe-DOTA-lisinopril quickly inactivated the N-domain of sACE-1 in the presence of H_2O_2 (without ascorbate), consistent with our previous observation that the respective M-chelates lacking lisinopril produce hydroxyl radicals in the presence of H_2O_2 but do not consume ascorbate.[44] Cu-EDTA-lisinopril was found to effectively inactivate sACE-1 in the presence of both ascorbate and H_2O_2 as its reduction potential lies between those of ascorbyl radical/ascorbate and $H_2O_2/OH^{\bullet}$.[26] For inactivation of the C-domain of sACE-1, each of the complexes Co-EDTA-lisinopril, Fe-DOTA-lisinopril, and Cu-DOTA-lisinopril showed a similar dependence on peroxide-promoted inactivation. In limited cases the introduction of ascorbate actually reduced the rate of sACE-1 inactivation, most likely due to the ability of ascorbate to scavenge ROS.

Our previous study with a fluorogenic substrate lacking domain selectivity, Mca-RPPGFSAFK(Dnp)-OH, illustrated that several M-chelate-lisinopril complexes not only promoted oxidative modifications but also cleaved sACE-1, since cleavage fragments were observed on SDS-PAGE.[30] Herein, we employed the N- and C-domain-selective substrates to investigate the enzyme activity at the individual domains, and we observed that the rates of inactivation of sACE-1 by M-chelate-lisinopril species were significantly dominant for the N-domain, as the ratios of rates of inactivation for the N-domain and C-domain (R_N/R_C) of sACE-1 were greater than 1 (Figure 7 and Supporting Information). In the presence of both ascorbate and peroxide, Cu-GGH-lisinopril illustrated the highest ratio of the inactivation rates at the N-domain to the C-domain (R_N/R_C) of sACE-1 shown in Figure 7, and our previous work also showed that under the same condition, Cu-GGH-lisinopril demonstrated the fastest cleavage rate of sACE-1, suggesting that the cleavage of sACE-1 may occur mainly at the N-domain.

Double-filter Effect

Herein we experimentally establish the double-filter effect, which results from the combination of binding selectivity and catalytic selectivity. The C/N double-filter selectivity factors (DFSF) are shown in Table 3 and were obtained from eqn. (1) as the product of the corresponding C/N domain binding selectivity factor (the ratio of inhibition constants $K_{i,N}$ / $K_{i,C}$, shown for each complex in Table 2) and the corresponding ratio of the rates of inactivation obtained at the C- and N-domain (the ratio R_C/R_N) under the same co-reactants conditions (inverse ratios R_N/R_C plotted in Figure 7 and in the Supporting Information).

$$\mathrm{DFSF} = (\mathrm{K_{i,N}}/\mathrm{K_{i,C}}) \times (\mathrm{R_C}/\mathrm{R_N}) \quad (1)$$

These numbers reflect the overall selectivity of irreversible inactivation for each catalyst. The catalysts Ni-GGH-lisinopril, Fe-EDTA-lisinopril, Co-EDTA-lisinopril, Ni-EDTA-lisinopril, Cu-EDTA-lisinopril, Fe-DOTA-lisinopril, Ni-DOTA-lisinopril, Cu-DOTA-lisinopril, Fe-CB-TE2A-lisinopril, and Cu-CB-TE2A-lisinopril each demonstrated greater catalytic efficiency (C/N double-filter selectivity factor) of inactivation of the C-domain than the N-domain, as shown in Table 3. For some catalysts, such as the Fe-NTA-lisinopril complex, a high C/N binding selectivity heavily influenced the C/N double-filter selectivity factor. In many cases, opposition of binding selectivity and catalytic selectivity resulted in balanced C/N double-filter selectivity factors (∼1). Complexes with the highest C/N double-filter selectivity factors may be the best candidates for selective irreversible inactivation of the C-domain of sACE-1, although successful use is also likely to require sufficiently high second-order rate constants for targeted inactivation.

CONCLUSIONS

We have developed a series of catalytic metallopeptides that target sACE-1. The catalysts showed a range of N- vs. C-domain binding selectivity, and reversible inhibition was typically selective toward the C-domain of sACE-1. The binding affinity of these lisinopril complexes appeared to correlate with size, charge (of the side chain), and hydrophobicity, with differences between the two domains causing selectivity. Catalytic inactivation by each of the M-chelate-lisinopril complexes was also monitored, and most complexes irreversibly inactivated sACE-1 at the N-domain more rapidly than at the C-domain, most likely reflecting that the reactivity depended on the alignment of each catalytic metal center, relative to the active site of each domain, and this alignment appeared more optimal for the N-domain. The combination of binding selectivity and catalytic selectivity resulted in a double-filter effect, in which efficient targeted inactivation required both targeted binding and a proper orientation of the metal center relative to the target once bound.[45] Additionally, the reactivity of these complexes demonstrated variable co-reactant selectivity that depended on the coordination environment, the reduction potential, and other factors. Our findings in this work will be useful for further development of domain-selective ACE inhibitors and are broadly applicable in the development of catalytic metallopeptides for selective inactivation of other protein targets.

EXPERIMENTAL SECTION

Enzyme

Recombinant human somatic ACE (sACE-1: Leu30-Leu1261, with C-terminal His tag, >95 % purity by SDS-PAGE under reducing conditions), originally isolated from an NS0-derived murine myeloma cell line, was purchased from R&D Systems. Single-use aliquots of sACE-1 were made and stored at −20 °C until use.

Substrates

Fluorogenic substrates Abz-SDK(Dnp)P-OH (N-domain-selective substrate) and Abz-LFK(Dnp)-OH (C-domain-selective substrate) were purchased from Enzo Life Science and Sigma Aldrich, respectively (Abz; aminobenzyl, Dnp; dinitrophenyl). Stocks of both

fluorogenic substrates were prepared in DMSO, and the concentrations were determined spectrophotometrically (using $\varepsilon_{365} = 17300$ M^{-1}cm^{-1}).[46]

Chemicals and Reagents

Lisinopril was purchased from Cayman Chemical Company. CB-TE2A and 1,4,7,10-tetraazacyclododecane-1,4,7,10-tetraacetic acid (DOTA) were purchased from Macrocyclics and stored at −20 °C in powder form. N-hydroxysuccinimide (NHS) was purchased from GenScript, and 1-ethyl-3-[3-dimethyl aminopropyl] carbodiimide hydrochloride (EDC) was purchased from Pierce and stored at −20 °C. Ethylenediaminetetraacetic acid (EDTA) was purchased from Aldrich. Nitrilotriacetic acid (NTA) was purchased from Sigma. The tripeptide GGH-OH (GGH) was obtained from Bachem. The Fe (II) sulfate heptahydrate, Co (II) chloride hexahydrate, Ni (II) acetate tetrahydrate, Cu (II) chloride dihydrate, and Zn (II) chloride salts were purchased from ACROS, J.T.Baker, Aldrich, J. T. Baker, and MCB Reagents, respectively. Sodium chloride, sodium hydroxide, and ammonium persulfate were purchased from Fisher. HEPES was purchased from Sigma. Acetonitrile, SDS, and Na$_2$HPO$_4$ were purchased from Sigma-Aldrich. NaHCO$_3$ was purchased from Mallinckrodt. The 40% acrylamide/Bis solution (19:1) was purchased from Bio-Rad, and TFA was purchased from ACROS. The C$_{18}$ preparatory and analytical columns used for RP-HPLC were purchased from Vydac. D$_2$O (99.96%) used for ^{1}H-NMR was purchased from Cambridge Isotopes Laboratory.

Synthesis and Characterization of Lisinopril-Coupled Chelates

The identities and purity of the synthesized chelate-lisinopril compounds (using EDTA, NTA, DOTA, GGH and CB-TE2A) were validated as previously reported. The synthesis of compound CB-TE2A-lisinopril was performed by first making a solution containing 500 mM CB-TE2A, 500 mM NHS, 500 mM EDC in DMSO and reacting for 20 min at ambient temperature. After 20 min, 48 μL of this reaction mixture was mixed with 552 μL of a solution that contained 22 mM lisinopril in 100 mM NaHCO$_3$, pH 8.0. The reaction proceeded overnight at RT in the dark, followed by HPLC purification. RP-HPLC elution conditions used a gradient method, running from 15 to 65% B from 0 to 45 min, 65 to 95% B from 45 to 50 min, and 95% B from 50 to 55 min where mobile phase A = H$_2$O, 0.1% TFA; B = acetonitrile, 0.1% TFA. The RP-HPLC fraction for product CB-TE2A-lisinopril was collected, lyophilized, resuspended in water, and ESI-TOF MS analysis provided the expected mass of 728.4 amu (negative mode) with no evidence of uncoupled lisinopril reactant (404 amu). The concentration of CB-TE2A-lisinopril was quantified by UV/vis titration with a solution containing a known concentration of copper (II) chloride. The lisinopril-coupled chelates used in these studies were > 99% purity as defined by RP-HPLC and ESI-MS.[33]

Preparation of Lisinopril-Conjugated Transition Metal Chelates

A 10 mM stock solution of each metal salt was prepared in water, except for the iron sulfate solution that was made fresh each day. The metal solution was added to each chelate-lisinopril compound in a buffer containing 20 mM HEPES, 100 mM NaCl, pH 7.4. The ratio of M: chelate-lisinopril was 1: 1.1, and the mixture was incubated at room temperature for at

least 30 min before use. The kinetic stability of M-CB-TE2A-lisinopril complexes was assessed as described earlier.[33]

Determination of Michaelis-Menten Kinetic Parameters (K_M and k_{cat}) for Domain-Selective Substrates

sACE-1 (1 nM) and variable concentrations of each fluorogenic substrate were incubated at 37 °C in a buffer containing 50 mM HEPES, 300 mM NaCl, 10 μM $ZnCl_2$, 0.05% Brij35, pH 7.4. The sACE-1-mediated hydrolysis of each fluorogenic substrate was monitored by measuring the increase in fluorescence at 420 nm (excitation wavelength at 320 nm). The observed fluorescent signal was corrected for inner filter effect (IFE) as shown in eqn. (2) where F_{obs} and F_{corr} are the uncorrected and corrected fluorescence intensities, respectively, c is the concentration of substrate, ℓ_{ex} and ℓ_{em} are the fluorescence cuvette pathlengths for excitation and emission, respectively, and ε_{ex} and ε_{em} are the fluorogenic substrate extinction coefficients at 320 nm and 420 nm, respectively.[47]

$$F_{corr} = F_{obs} . 10^{\wedge}[(\varepsilon_{ex}.\ell_{ex} + \varepsilon_{em}.\ell_{em}).c/2] \quad (2)$$

The initial slope for each trace (RFU/min) was converted into concentration units (μM/min) based on a calibration curve obtained from the complete hydrolysis of several concentrations of each corresponding substrate.

Determination of IC$_{50}$ Values

sACE-1 (1 nM) and variable concentrations of each M-chelate-lisinopril complex were preincubated for 20 min at 37 °C in a buffer containing 50 mM HEPES, 300 mM NaCl, 10 μM $ZnCl_2$, 0.05% Brij35, pH 7.4. After preincubation, 1.4 μL of 0.5 mM fluorogenic substrate was added into 68.6 μL of the mixture and substrate cleavage by sACE-1 was immediately monitored by real-time fluorimetry at 37 °C, with excitation at 320 nm and emission at 420 nm. Initial rates of fluorescence increase were determined for each concentration of M-chelate-lisinopril, and these initial rates were expressed as a percentage (% maximal activity) of the average of several initial rates of uninhibited substrate cleavage by sACE-1 in the absence of M-chelate-lisinopril complexes (using the same substrate). Plots of % maximal activity vs. M-chelate-lisinopril concentration were fit to eqn. (3), where A, [I], n, and [IC$_{50}$] are the % maximal activity, inhibitor concentration, fitted cooperativity, and fitted IC$_{50}$ respectively. For each M-chelate-lisinopril complex, IC$_{50}$ values were determined for each domain, by use of the corresponding domain-selective substrates.

$$A = (100\%)/[1 + ([I]/[IC_{50}])^n] \quad (3)$$

Determination of Inhibition Mode by Dixon Plots

First, sACE-1 (1 nM) was preincubated with variable concentrations of inhibitor for 20 min at 37 °C in a buffer containing 50 mM HEPES, 300 mM NaCl, 10 μM $ZnCl_2$, 0.05% Brij35, pH 7.4. Second, variable concentrations of each fluorogenic substrate were added into the preincubated mixture and the fluorescence traces were immediately monitored. The concentrations of the substrates Abz-SDK(Dnp)P-OH and Abz-LFK(Dnp)-OH were 7.5, 10

and 15 μM. The observed fluorescent signal was corrected for IFE using eqn. (2)[47] and the initial rates (μM/min) for all traces were calculated as described above. Dixon plots were created by plotting the reciprocal initial rate (min/μM) vs. the concentration of inhibitor, for each substrate concentration. The inhibition constant (K_i) for reversible binding of each inhibitor to each domain was calculated from eqn. (4) for the classical competitive inhibitor, where IC_{50}, [S] and K_M are the inhibitor concentration that gave half-maximal activity, the substrate concentration, and the Michaelis constant, respectively.[48,49]

$$K_i = IC_{50}/(1+[S]/K_M) \quad (4)$$

Time-Dependent Inactivation of sACE-1

sACE-1 and each M-chelate-lisinopril complex were preincubated for 20 min at 37 °C in a buffer containing 50 mM HEPES, 300 mM NaCl, 10 μM ZnCl$_2$, 0.05% Brij35, pH 7.4. After preincubation, co-reactants ascorbate and/or H$_2$O$_2$ (or no co-reactants) were added to initiate each reaction. Reaction concentrations were 1 nM sACE-1, a concentration of M-chelate-lisinopril that gave ~80% activity (calculated by use of eqn. (3), where A = 80%), and 1 mM ascorbate and/or H$_2$O$_2$ (or no co-reactants). Each time-dependent ACE-inactivation reaction proceeded at 37 °C for a period of 2 h, and at each specific intervening time point, a 68.6 μL aliquot was taken from the reaction mixture and mixed with 1.4 μL of 0.5 mM fluorogenic substrate in a fluorescence cuvette. Substrate cleavage by sACE-1 was immediately monitored by real-time fluorimetry as described above. Initial rates of substrate cleavage were determined for each time point for the time-dependent inactivation of sACE-1, and these initial rates were expressed as a percentage (% maximal activity) of the average of several initial rates for uninhibited substrate cleavage by sACE-1 (same substrate), determined in the absence of both inhibitor and co-reactants. Plots of % maximal activity vs. time were fit to a first-order exponential decay model (eqn. (5)), and the initial rate of inactivation of sACE-1 by each M-chelate-lisinopril complex was determined. Experiments were performed for each domain-selective substrate (for each catalyst with or without co-reactants).

$$y = Ae^{-kx} + y_0 \quad (5)$$

Supplementary Material

Refer to Web version on PubMed Central for supplementary material.

Acknowledgments

ABBREVIATIONS USED

Abz	aminobenzoic acid
Dnp	dinitrophenol
DFSF	double-filter selectivity factors
DOTA	1,4,7,10-tetraazacyclododecane-1,4,7,10-tetraacetic acid
EDC	1-ethyl-3-[3-dimethyl aminopropyl] carbodiimide hydrochloride
NHS	N-hydroxysuccinimide
NTA	nitrilotriacetic acid

REFERENCES

1. Brown NJ, Vaughan DE. Angiotensin-converting enzyme inhibitors. Circulation. 1998; 97:1411–1420. [PubMed: 9577953]

2. Skidgel, RA.; Erdos, EIn. The Renin-Angiotensin System. Robertson, JIS.; Nicholls, MG., editors. Raven Press Ltd: New York, NY; 1993. p. 10.11-10.10

3. Ehlers MR, Riordan JF. Angiotensin-converting enzyme: new concepts concerning its biological role. Biochemistry. 1989; 28:5311–5318. [PubMed: 2476171]

4. Folkow B, Johansson B, Mellander S. The comparative effects of angiotensin, noradrenaline on consecutive vascular sections. Acta Physiol. Scand. 1961; 53:99–104. [PubMed: 13893844]

5. Erdös EG. The angiotensin Iconverting enzyme. Fed. Proc. 1977; 36:1760–1765. [PubMed: 191298]

6. Wei L, Alhenc-Gelas F, Corvol P, Clauser E. The two homologous domains of human angiotensin I-converting enzyme are both catalytically active. J. Biol. Chem. 1991; 266:9002–9008. [PubMed: 1851160]

7. Villard E, Soubrier F. Molecular biology genetics of the angiotensin-I-converting enzyme: potential implications in cardiovascular diseases. Cardiovasc. Res. 1996; 32:999–1007. [PubMed: 9015402]

8. Regoli D, Barabé J. Pharmacology of bradykinin and related kinins. Pharmacol. Rev. 1980; 32:1–46. [PubMed: 7015371]

9. Kumar RS, Kusari J, Roy SN, Soffer RL, Sen GC. Structure of testicular angiotensin-converting enzyme. A segmental mosaic isozyme. J. Biol. Chem. 1989; 264:16754–16758. [PubMed: 2550457]

10. Natesh R, Schwager SL, Sturrock ED, Acharya KR. Crystal structure of the human angiotensin-converting enzyme-lisinopril complex. Nature. 2003; 421:551–554. [PubMed: 12540854]

11. Corradi HR, Schwager SL, Nchinda AT, Sturrock ED, Acharya KR, Crystal KR. Crystal structure of the N domain of human somatic angiotensin I-converting enzyme provides a structural basis for domain-specific inhibitor design. J. Mol. Biol. 2006; 357:964–974. [PubMed: 16476442]

12. Jaspard E, Wei L, Alhenc-Gelas F. Differences in the properties and enzymatic specificities of the two active sites of angiotensin I-converting enzyme (kininase II). Studies with bradykinin and other natural peptides. J. Biol. Chem. 1993; 268:9496–9503. [PubMed: 7683654]

13. Ceconi C, Francolini G, Olivares A, Comini L, Bachetti T, Ferrari R. Angiotensin-converting enzyme (ACE) inhibitors have different selectivity for bradykinin binding sites of human somatic ACE. Eur. J. Pharmacol. 2007; 577:1–6. [PubMed: 17716647]

14. Araujo MC, Melo RL, Cesari MH, Juliano MA, Juliano L, Carmona AK. Peptidase specificity characterization of C- and N-terminal catalytic sites of angiotensin I-converting enzyme. Biochemistry. 2000; 39:8519–8525. [PubMed: 10913258]

15. Junot C, Gonzales MF, Ezan E, Cotton J, Vazeux G, Michaud A, Azizi M, Vassiliou S, Yiotakis A, Corvol P, Dive V. RXP 407, a selective inhibitor of the N-domain of angiotensin I-converting enzyme, blocks in vivo the degradation of hemoregulatory peptide acetyl-Ser-Asp-Lys-Pro with no effect on angiotensin I hydrolysis. J. J. Pharmacol. Exp. Ther. 2001; 297:606–611. [PubMed: 11303049]

16. Jullien ND, Cuniasse P, Georgiadis D, Yiotakis A, Dive V. Combined use of selective inhibitors and fluorogenic substrates to study the specificity of somatic wild-type angiotensin-converting enzyme. FEBS J. 2006; 273:1772–1781. [PubMed: 16623712]

17. Georgiadis D, Cuniasse P, Cotton J, Yiotakis A, Dive V. Structural determinants of RXPA380, a potent and highly selective inhibitor of the angiotensin-converting enzyme C-domain. Biochemistry. 2004; 43:8048–8054. [PubMed: 15209500]

18. Wei L, Clauser E, Alhenc-Gelas F, Corvol P. The two homologous domains of human angiotensin I-converting enzyme interact differently with competitive inhibitors. J. Biol. Chem. 1992; 267:13398–13405. [PubMed: 1320019]

19. Voronov S, Zueva N, Orlov V, Arutyunyan A, Kost O. Temperature-induced selective death of the C-domain within angiotensin-converting enzyme molecule. FEBS Lett. 2002; 522:77–82. [PubMed: 12095622]

20. Deddish PA, Marcic B, Jackman HL, Wang HZ, Skidgel RA, Erdös EG. N-domain-specific substrate and C-domain inhibitors of angiotensin-converting enzyme: angiotensin-(1-7) and keto-ACE. Hypertension. 1998; 31:912–917. [PubMed: 9535414]

21. Robinson S, Lenfant M, Wdzieczak-Bakala J, Melville J, Riches A. The mechanism of action of the tetrapeptide acetyl-N-Ser-Asp-Lys-Pro (AcSDKP) in the control of haematopoietic stem cell proliferation. Cell. Prolif. 1992; 25:623–632. [PubMed: 1457609]

22. Rousseau A, Michaud A, Chauvet MT, Lenfant M, Corvol P. The hemoregulatory peptide N-acetyl-Ser-Asp-Lys-Pro is a natural and specific substrate of the N-terminal active site of human angiotensin-converting enzyme. J. Biol. Chem. 1995; 270:3656–3661. [PubMed: 7876104]

23. Bogden AE, Carde P, de Paillette ED, Moreau JP, Tubiana M, Frindel E. Amelioration of chemotherap-induced toxicity by cotreatment with AcSDKP, a tetrapeptide inhibitor of hematopoietic stem cell proliferation. Ann. N. Y. Acad. Sci. 1991; 628:126–139. [PubMed: 1648882]

24. Esther CR, Marino EM, Howard TE, Machaud A, Corvol P, Capecchi MR, Bernstein KE. The critical role of tissue angiotensin-converting enzyme as revealed by gene targeting in mice. J. Clin. Invest. 1997; 99:2375–2385. [PubMed: 9153279]

25. Hocharoen L, Cowan JA. Metallotherapeutics: novel strategies in drug design. Chem. Eur. J. 2009; 15:8670–8676. [PubMed: 19685535]

26. Joyner JC, Cowan JA. Targeted cleavage of HIV RRE RNA by Rev-coupled transition metal chelates. J. Am. Chem. Soc. 2011; 133:9912–9922. [PubMed: 21585196]

27. Gokhale NH, Bradford S, Cowan JA. Stimulation and oxidative catalytic inactivation of thermolysin by copper. Cys-Gly-His-Lys. J. Biol. Inorg. Chem. 2007; 12:981–987. [PubMed: 17618468]

28. Jin Y, Lewis MA, Gokhale NH, Long EC, Cowan JA. Influence of stereochemistry and redox potentials on the single- and double-strand DNA cleavage efficiency of Cu(II) and Ni(II) Lys-Gly-His-derived ATCUN metallopeptides. J. Am. Chem. Soc. 2007; 129:8353–8361. [PubMed: 17552522]

29. Joyner JC, Keuper KD, Cowan JA. DNA nuclease activity of Rev-coupled transition metal chelates. Dalt. Trans. 2012; 41:6567–6578.

30. Joyner JC, Hocharoen L, Cowan JA. Targeted catalytic inactivation of angiotensin converting enzyme by lisinopril-coupled transition-metal chelates. J. Am. Chem. Soc. 2012; 134:3396–3410. [PubMed: 22200082]

31. Bersanetti PA, Andrade MC, Casarini DE, Juliano MA, Nchinda AT, Sturrock ED, Juliano L, Carmona AK. Positional-scanning combinatorial libraries of fluorescence resonance energy transfer peptides for defining substrate specificity of the angiotensin I-converting enzyme and development of selective C-domain substrates. Biochemistry. 2004; 43:15729–15736. [PubMed: 15595828]

32. Joyner JC, Cowan JA. Targeted Cleavage of HIV RRE RNA by Rev Coupled Transition Metal Chelates. J. Am. Chem. Soc. 2011; 133:9912–9922. [PubMed: 21585196]

33. Joyner JC, Hocharoen L, Cowan JA. Targeted catalytic inactivation of angiotensin converting enzyme by lisinopril-coupled transition-metal chelates. J. Am. Chem. Soc. 2012; 134:3396–3410. [PubMed: 22200082]

34. Fernandez JH, Hayashi MA, Camargo AC, Neshich G. Structural basis of the lisinopril-binding specificity in N- and C-domains of human somatic ACE. Biochem. Biophys. Res. Commun. 2003; 308:219–226. [PubMed: 12901857]

35. Savelli G, Spreti N, Di Profio P. Enzyme activity and stability control by amphiphilic self-organizing systems in aqueous solutions. Curr. Opin. Colloid Interface Sci. 2000; 5:111–117.

36. Gebicka L, Jurgas-Grudzinska M. Activity and stability of catalase in nonionic micellar and reverse micellar systems. Z. Naturforsch C. 2004; 59:887–891. [PubMed: 15666551]

37. Tzakos AG, Galanis AS, Spyroulias GA, Cordopatis P, Manessi-Zoupa E, Gerothanassis IP. Structure-function discrimination of the N- and C-catalytic domains of human angiotensin-converting enzyme: implications for Cl- activation and peptide hydrolysis mechanisms. Protein Eng. 2003; 16:993–1003. [PubMed: 14983080]

38. Nakamura Y, Yamamoto N, Sakai K, Okubo A, Yamazaki S, Takano T. Purification and characterization of angiotensin I-converting enzyme inhibitors from sour milk. J. Dairy Sci. 1995; 78:777–783. [PubMed: 7790570]

39. Ondetti MA, Rubin B, Cushman DW. Design of specific inhibitors of angiotensin-converting enzyme: new class of orally active antihypertensive agents. Science. 1977; 196:441–444. [PubMed: 191908]

40. Fuglsang A, Nilsson D, Nyborg NC. Characterization of new milk-derived inhibitors of angiotensin converting enzyme in vitro and in vivo. J. Enzyme Inhib. Med. Chem. 2003; 18:407–412. [PubMed: 14692507]

41. Graf E, Mahoney JR, Bryant RG, Eaton JW. Iron-catalyzed hydroxyl radical formation. Stringent requirement for free iron coordination site. J. Biol. Chem. 1984; 259:3620–3624. [PubMed: 6323433]

42. Buettner GR, Jurkiewicz BA. Catalytic metals, ascorbate and free radicals: combinations to avoid. Radiat. Res. 1996; 145:532–541. [PubMed: 8619018]

43. Chiou SH. DNA-scission and protein-scission activities of ascorbate in the presence of copper-ion and a copper-peptide complex. J. Biochem. 1983; 94:1259–1267. [PubMed: 6654857]

44. Joyner JC, Reichfield J, Cowan JA. Factors influencing the DNA nuclease activity of iron, cobalt, nickel, and copper chelates. J. AmChem. Soc. 2011; 133:15613–15626.

45. Cowan JA. Catalytic MetalloDrugs. Pure App. Chem. 2008; 80:1799–1810.

46. Carmona AK, Schwager SL, Juliano MA, Juliano L, Sturrock ED. A continuous fluorescence resonance energy transfer angiotensin I-converting enzyme assay. Nat. Protoc. 2006; 1:1971–1976. [PubMed: 17487185]

47. Palmier MO, Van Doren SR. Rapid determination of enzyme kinetics from fluorescence: overcoming the inner filter effect. Anal. Biochem. 2007; 371:43–51. [PubMed: 17706587]

48. Burlingham BT, Widlanski TS. An intuitive look at the relationship of K-i and IC50: A more general use for the Dixon plot. J. Chem. Educ. 2003; 80:214–218.

49. Cer RZ, Mudunuri U, Stephens R, Lebeda FJ. IC50-to-Ki: a web-based tool for converting IC50 to Ki values for inhibitors of enzyme activity and binding. Nucleic Acids Res. 2009; 37:W441–W445. [PubMed: 19395593]

Figure 1.
Summary of the M-chelate-lisinopril complexes. M = Fe^{3+}, Co^{2+}, Ni^{2+}, Cu^{2+}; R = N(H)-lisinopril. Reduction potentials of the M-chelate domains were determined previously,[32] and redox couples are 3+/2+ for Fe, Co, Ni-ATCUN, and Cu-ATCUN complexes and 2+/1+ for all other Ni and Cu complexes.
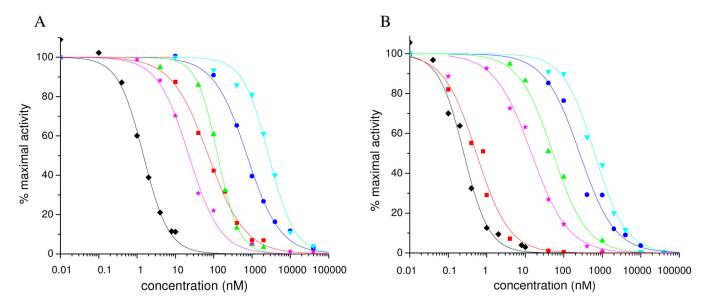
Figure 2.
Concentration-dependent inhibition of sACE-1 using (A) the N-domain-selective substrate, Abz-SDK(Dnp)P-OH, and (B) the C-domain-selective substrate, Abz-LFK(Dnp)-OH. Dose-response curves are shown for lisinopril (♦), NTA-lisinopril (■), GGH-lisinopril (▲), EDTA-lisinopril (●), DOTA-lisinopril (▼), and CB-TE2A-lisinopril (★).
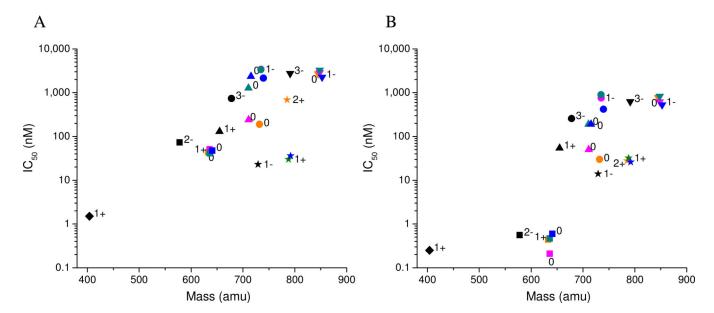
Figure 3.
Relationship between IC$_{50}$ values and both the charge of side chain and mass of M-chelate-lisinopril complexes using (A) the N-domain-selective substrate, Abz-SDK(Dnp)P-OH, and (B) the C-domain-selective substrate, Abz-LFK(Dnp)-OH. Plots include lisinopril (♦) and metal complexes of NTA-lisinopril (■), GGH-lisinopril (▲), EDTA-lisinopril (●), DOTA-lisinopril (▼), and CB-TE2A-lisinopril (★). Orange, Fe; pink, Co; green, Ni; blue, Cu; black, no metal.
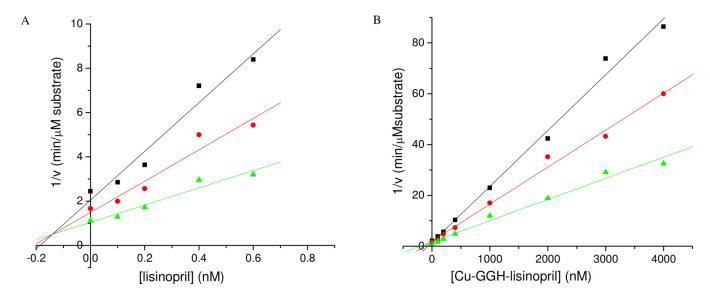
Figure 4.
Dixon plots of sACE-1 with (A) lisinopril and (B) Cu-GGH-lisinopril with various concentrations of the C-domain-selective substrate, Abz-LFK(Dnp)-OH: 7.5 μM (■), 10 μM (♦) and 15 μM (▲). The correlation coefficients for the lines in (A) are 0.96, 0.94, and 0.95 and for lines in (B) are 0.99, 0.99, and 0.98 for substrate concentration = 7.5 μM, 10 μM, and 15 μM, respectively.
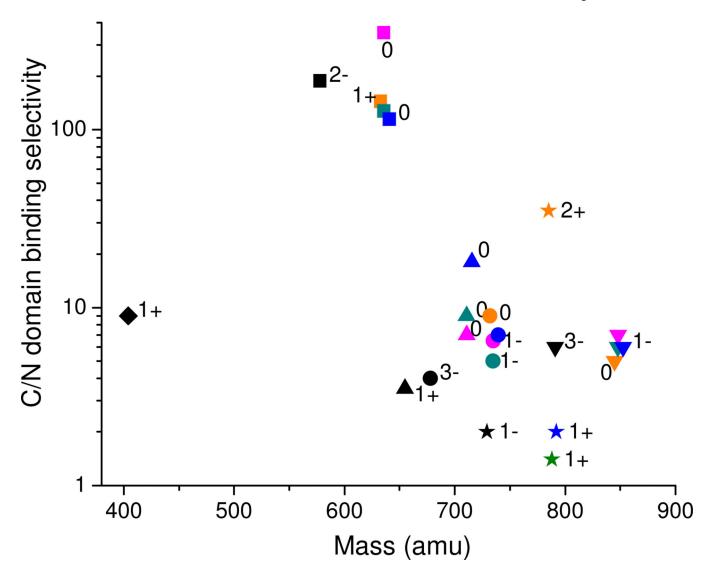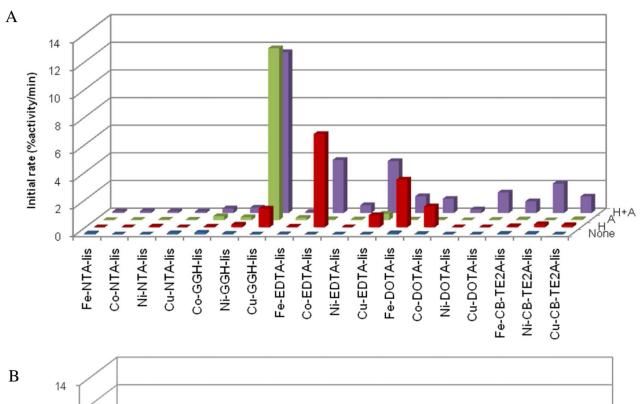
Figure 5.
C/N domain binding selectivity factors were influenced primarily by the identity of the chelating ligand (the data within the plot were typically clustered into ligand-specific regions) and also by the size, charge, shape, and hydrophobicity of the resulting coordination complexes. The data shown here include lisinopril (♦) and both metal-free and metal-bound forms of NTA-lisinopril (■), GGH-lisinopril (▲), EDTA-lisinopril (●), DOTA-lisinopril (▼) and CB-TE2A-lisinopril (★). Orange, Fe; pink, Co; green, Ni; blue, Cu; black, no metal.

A

B
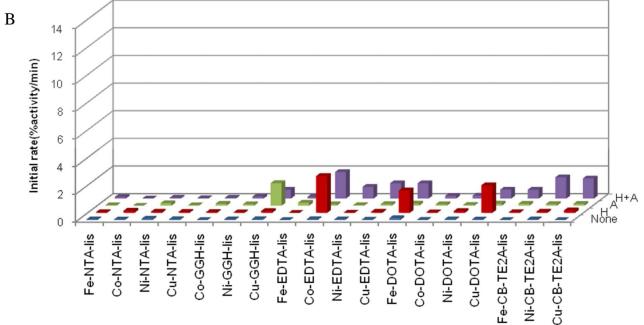
Figure 6.
Initial rates of inactivation of each domain (R_N and R_C) of sACE-1 by M-chelate-lisinopril complexes and co-reactants, monitored by use of (A) the N-domain-selective substrate, Abz-SDK(Dnp)P-OH and (B) the C-domain-selective substrate, Abz-LFK(Dnp)-OH. The co-reactants used (1 mM each) were H_2O_2 + ascorbate (H+A), ascorbate (A), H_2O_2 (H), or no co-reactant (None).
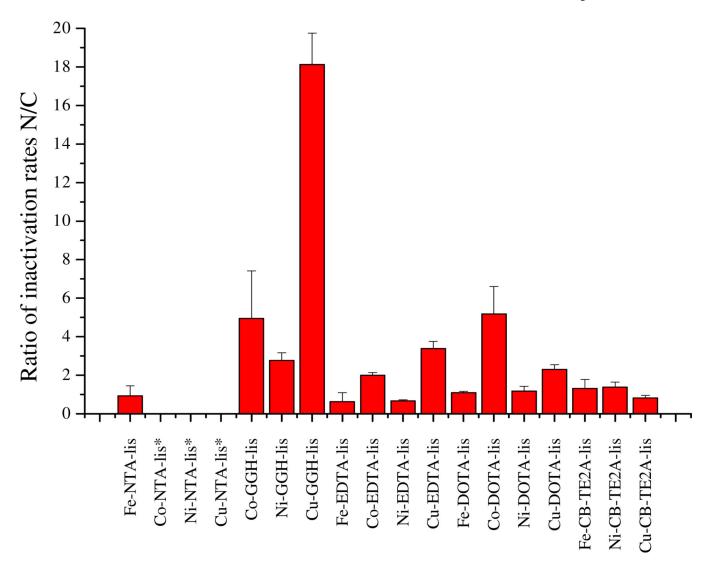
Figure 7.
Ratios of the inactivation rates for the N/C domains (R_N/R_C) for each metal-chelate-lisinopril complexes, obtained when both ascorbate and peroxide were present.
*undetermined due to large uncertainty.

Table 1

Apparent Michaelis-Menten kinetic parameters of different substrates used by sACE-1

Substrate	k_{cat} (min^{-1})	K_M (μM)	k_{cat} / K_M (μM^{-1} min^{-1})
Mca-RPPGFSAFK(Dnp)-OH[a]	1220 ± 50	4.5 ± 0.6	270 ± 40
Abz-SDK(Dnp)P-OH	180 ± 10	35 ± 5	5 ± 1
Abz-LFK(Dnp)-OH	1380 ± 90	12 ± 2	115 ± 20

[a]see ref [30]

Table 2

IC_{50} and K_i values for inhibition of the N- and C-domains of sACE-1 and domain selectivity factors for reversible inhibition by each M-chelate-lisinopril complex.

Complex[a]	IC_{50} (nM)		K_i (nM)		C/N domain selectivity factor[b]
	With Abz-SDK(Dmp)P-OH, (N-domain)	With Abz-LFK(Dmp)-OH, (C-domain)	With Abz-SDK(Dmp)P-OH, (N-domain)	With Abz-LFK(Dmp)-OH, (C-domain)	
[NTA]$^{2-}$–lisin	73 ± 4	0.56 ± 0.06	57 ± 3	0.31 ± 0.05	180 ± 30
[Fe-NTA]$^{1+}$-lisin	44 ± 3	0.44 ± 0.04	35 ± 2	0.24 ± 0.04	140 ± 20
[Co-NTA]^0-lisin	51 ± 3	0.21 ± 0.03	40 ± 2	0.12 ± 0.03	350 ± 60
[Ni-NTA]^0–lisin	42 ± 4	0.47 ± 0.02	33 ± 3	0.26 ± 0.02	130 ± 20
[Cu-NTA]^0–lisin	48 ± 1	0.6 ± 0.08	38 ± 1	0.33 ± 0.07	120 ± 20
[GGH]$^{1-}$-lisin	130 ± 5	54 ± 4	102 ± 4	29 ± 4	3.5 ± 0.5
[Co-GGH]^0-lisin	240 ± 6	50 ± 2	189 ± 5	27 ± 3	6.9 ± 0.6
[Ni-GGH]^0-lisin	1,300 ± 200	210 ± 20	1000 ± 100	110 ± 20	9 ± 2
[Cu-GGH]^0-lisin	2,300 ± 500	190 ± 10	1900 ± 400	100 ± 10	18 ± 4
[EDTA]$^{3-}$lisin	740 ± 50	257 ± 36	580 ± 40	140 ± 30	4 ± 1
[Fe-EDTA]^0-lisin	190 ± 7	30 ± 3	150 ± 6	16 ± 3	9 ± 1
[Co-EDTA]$^{1-}$-lisin	3,400 ± 300	760 ± 20	2700 ± 200	410 ± 40	6.5 ± 0.7
[Ni-EDTA]$^{1-}$-lisin	3,400 ± 600	900 ± 100	2600 ± 500	490 ± 90	5 ± 1
[Cu-EDTA]$^{1-}$-lisin	2,100 ± 200	420 ± 30	1700 ± 100	230 ± 30	7 ± 1
[DOTA]$^{1-}$-lisin	2,700 ± 200	629 ± 55	2200 ± 200	340 ± 50	6 ± 1
[Fe-DOTA]^0-lisin	2,700 ± 80	780 ± 60	2130 ± 70	420 ± 60	5.0 ± 0.6
[Co-DOTA]$^{1-}$-lisin	2,900 ± 200	620 ± 140	2300 ± 100	300 ± 100	7 ± 1
[Ni-DOTA]$^{1-}$-lisin	3,300 ± 300	830 ± 70	2600 ± 200	450 ± 60	6 ± 1
[Cu-DOTA]$^{1-}$-lisin	2,300 ± 300	530 ± 50	1800 ± 200	290 ± 40	6 ± 1
[CB-TE2A]$^{1-}$-lisin	23 ± 2	14 ± 2	18 ± 1	8 ± 2	2.2 ± 0.6
[Fe-CB-TE2A]$^{2+}$-lisin	690 ± 10	28 ± 5	540 ± 10	15 ± 4	40 ± 10
[Ni-CB-TE2A]$^{1+}$-lisin	30 ± 5	32 ± 1	23 ± 4	17 ± 2	1.4 ± 0.3

Complex[a]	IC$_{50}$ (nM)		K$_i$ (nM)		C/N domain selectivity factor[b]
	With Abz-SDK(Dnp)P-OH, (N-domain)	With Abz-LFK(Dnp)-OH, (C-domain)	With Abz-SDK(Dnp)P-OH, (N-domain)	With Abz-LFK(Dnp)-OH, (C-domain)	
[Cu-CB-TE2A]$^{1+}$-lisin	36 ± 6	26 ± 4	28 ± 5	14 ± 3	2.0 ± 0.6
Lisinopril	1.5 ± 0.1	0.25 ± 0.02	1.0 ± 0.1	0.10 ± 0.01	9 ± 1

[a] lisin = lisinopril,

[b] C/N selectivity factor = ratio of K$_i$ for N-domain to K$_i$ for C-domain (K$_i$,N/K$_i$,C).

Table 3

C/N double-filter selectivity factors (DFSF)[a]

Complexes[b]	A+H[c]
[Fe-NTA]$^{1+}$–lisin	160 ± 90
[Co-NTA]^{0}–lisin	__[d]
[Ni-NTA]^{0}–lisin	__[d]
[Cu-NTA]^{0}–lisin	__[d]
[Co-GGH]^{0}–lisin	1.4 ± 0.7
[Ni-GGH]^{0}–lisin	3.2 ± 0.8
[Cu-GGH]^{0}–lisin	1.0 ± 0.2
[Fe-EDTA]$^{0-}$–lisin	__[d]
[Co-EDTA]$^{1-}$–lisin	3.2 ± 0.4
[Ni-EDTA]$^{1-}$–lisin	8 ± 2
[Cu-EDTA]$^{1-}$–lisin	2.2 ± 0.4
[Fe-DOTA]^{0}–lisin	4.6 ± 0.6
[Co-DOTA]$^{1-}$–lisin	1.3 ± 0.5
[Ni-DOTA]$^{1-}$–lisin	5 ± 1
[Cu-DOTA]$^{1-}$–lisin	2.7 ± 0.6
[Fe-CB-TE2A]$^{2+}$-lisin	30 ± 10
[Ni-CB-TE2A]$^{1+}$–lisin	1.0 ± 0.3
[Cu-CB-TE2A]$^{1+}$–lisin	2.4 ± 0.8

[a] calculated using eqn. (5) (Experimental Section).

[b] lisin=lisinopril.

[c] In the presence of 1 mM ascorbate + 1 mM H_2O_2.

[d] undetermined due to large uncertainty.